11th International Symposium on Rock Fragmentation by Blasting

Paper Number: 152

Effects of joint intensity on rock fragmentation by impact

S. Aziznejad[1] and K. Esmaieli[2]

1.
MASc. candidate, University of Toronto, Lassonde Institute of Mining, Toronto, Canada. Email: sh.aziznejad@mail.utoronto.ca

2.
Assistant Professor, University of Toronto, Lassonde Institute of Mining, Toronto, Canada, Email: Kamran.esmaeili@utoronto.ca

ABSTRACT

Impact-induced rock fragmentation is a mechanism that is commonly used for rock breakage in drilling and crushing. Additionally, rock fragmentation by blasting is frequently used in rock excavation operations. Experience shows that presence of discontinuities in rock can significantly influence the impact-induced damage and fragmentation of rock. Quantification of the response of jointed rock masses to impact loads is complicated by the fact that the available laboratory tests are mainly designed for aggregates or intact rocks. It can be argued that neither of these tests adequately represent a jointed rock mass. This paper presents the results of a series of numerical simulations used to investigate the influence of pre-existing discontinuities on the impact-induced fragmentation of rock masses. The methodology includes determination of the static and dynamic mechanical properties of a rock unit by conducting a series of laboratory tests on intact rock samples collected from a quarry in Canada. A 2D distinct element code, Particle Flow Code (PFC2D), was used to generate a bonded particle model in order to simulate both static mechanical properties (Uniaxial Compressive Strength, Elastic Modulus, Poisson's Ratio and indirect Tensile Strength) and dynamic mechanical property (drop weight tensile strength) of the intact rock. The calibrated numerical model was then used to construct large-scale synthetic rock mass samples by incorporating discontinuity networks of different intensity into the bonded particle model. Finally, the impact-induced fragmentation inflicted by a rigid projectile particle on the jointed rock mass samples, simulated by a synthetic rock mass model, was determined. More fragmentation was observed for the rock mass samples with higher joint intensity.

INTRODUCTION

In many mining and civil engineering applications drilling and blasting are used for rock excavation. Rock fragmentation through impact loading is of particular interest in these cases. In a percussive drilling process, the rock material is broken by drilling bit through continuous hitting of the rock material in a hole. Similarly, in blasting, rock material is subjected to shock produced by explosives. An efficient drilling and blasting operation allows producing of optimum size of rock fragments, demanding less amounts of crushing energy. Impact induced rock fragmentation mechanism is also used in crushers for rock breakage. Impact crushers involve the use of dynamic impact loading during comminution process. Comminution is generally the most energy intensive process in mining. Hence, investigation of rock mass behaviour under dynamic impact loading allows for a better understanding of energy dissipation in drilling, blasting, and crushing process and consequently a more reliable prediction of rock fragmentation.

Laboratory tests have been commonly used to quantify the response of rock materials to impact loading and to investigate the mechanism of rock fragmentation, (Wagner and Schumann 1971; Hustrulid and Fairhurst 1972; Lindqvist 1982; Cook et al. 1984; Pang and Goldsmith 1990; Lindqvist et al. 1994; Mishnaevsky Jr 1995; Kou 1995; Camacho and Ortiz, 1996; Prasad et al. 2000; Momber, 2003; Gao et al., 2010; Cao et al., 2011; Nariseti et al. 2012). These laboratory experiments have played an essential role in understanding of rock fragmentation phenomena and to establish models to study failure mechanisms of rocks subjected to impact loading. However, due to anisotropy and inhomogeneity of tested rock materials, the process of fracture initiation and propagation has not been fully understood in the laboratory tests. The impact induced rock fragmentation is the results of damage evolution that starts with initiation of microcracks in rock, which is followed by growth and coalescence of these microcracks. Some researchers have focused on development of theoretical models, within the framework of continuum damage mechanics, for studying the evolution of rock damage under impact loading, and the mechanism of rock fragmentation (Grady and Kipp, 1980; Taylor et al., 1986; Kuszmaul, 1987; Throne et al., 1990; Ahrens and Rubin, 1993; Hu and Li, 2006). In most of these analytical models there are too many parameters involved, and it is generally difficult to quantify all of them. Numerical modeling tools have also been used to determine the behavior of rock materials under impact loading, (Wang and Lehnhoff, 1976; Kumano, 1980; Taylor et al., 1986; Beus et al., 1999; Nazeri et al., 2002; Liu, 2004; Han et al., 2005; Wang and Tonon, 2010; Gao et al. 2010). Most of these investigations have focused on the response of rock material to impact loading. Limited studies have been carried out to understand the role of pre-existing discontinuities in rock mass damage by impact.

This paper presents the results of a series of numerical simulations that aims to contribute to our understanding of the influence of joint intensity on the response of rock masses to impact loading. The 2D Particle Flow Code, a distinct element code developed by Itasca (2013), was used to simulate static and dynamic mechanical properties of a meta-sandstone rock unit. The calibrated numerical model was subsequently used for generation of large scale rock mass samples with different joint intensity. Jointed rock mass samples were then subjected to impact loading. This allowed quantification of damage and fragmentation inflicted in each rock mass sample.

EXPERIMENTAL TESTS

Rock samples of a Meta-sandstone rock unit from a quarry in Nova Scotia, Canada were collected and tested at CanmetMINING Rock Mechanics Laboratory. The samples were subjected to both static and dynamic tests including uniaxial compression test, static Brazilian indirect tensile strength test, and dynamic drop test. To determine the dynamic tensile strength of rock samples, dynamic drop tests were carried out using a vertical impact load frame Dynatup® Model 9210. Drop tests were carried out with an impact weight of 19.35 kg, a drop height of 46 cm, for a total potential energy of 87 Joules (J) in the system, and an impact velocity of 3 m/s. The static mechanical properties (i.e. Uniaxial Compressive Strength, Elastic Modulus, Poisson's Ratio, and indirect Tensile Strength), and dynamic mechanical property (dynamic tensile strength) of the intact rock are summarized in Table 1. The number of samples used for each type of test and the mean and standard deviation of the measured properties are given.

NUMERICAL MODELING

Simulation of intact rock properties

To simulate the intact rock properties measured in the laboratory, a bonded particle model (BPM) was used. The BPM was first developed by Potyondy and Cundall in 2004, and is based on the Particle Flow Code. In a two dimensional BPM, an intact rock is simulated as an assembly of rigid distinct circular particles, bonded together at their contact points. A linear contact and a frictional sliding model is used to describe the physical behavior of the contacts. The intact rock sample was generated using procedure developed by Potyondy and Cundall (2004). First a material vessel with the same dimensions as the laboratory test samples (12 cm height and 5 cm of width) was created. The circular balls were randomly generated in the vessel to match the target porosity of the intact rock (5%). A minimum particle size of 0.3 mm was used which is close to the minimum grain size of the rock samples. To remove kinetic energy from the balls in the vessel and allow them to reach an equilibrium condition, the density and local damping coefficient were assigned to the balls. Once a dense packing of circular particles was achieved, all contacts between the circular particles were bonded using the recently developed flat-joint contact model, (Potyondy, 2012). The flat-joint contact model simulates the contact interface between two circular balls with a locally flat notional surface. A failure in the BPM is simulated as the break of bonded segments in the interface. The advantages of the flat-joint contact model over other contact models such as parallel bonds is that even after the bond failure, the interface continues to resist against relative rotation. This allows a higher ratio of compressive strength to tensile strength, which is an important characteristics of hard brittle rocks, be achieved, Potyondy (2012).

An inverse calibration method was employed to establish the appropriate micro-properties which consist of strength and stiffness parameters for balls and contacts for generation of the BPM that would replicate the representative intact rock properties.

To simulate the dynamic drop test, a disk shape BPM was put in contact with a frictionless bottom rigid wall. The upper drop plate was simulated using the clump logic. The properties of the drop plate clump are summarized in Table 2. The disc shape sample was loaded by dropping the plate toward the sample. During the test, the impact force acting on the sample was monitored, and the maximum value was used to calculate the dynamic tensile strength of rock. For calibration of the dynamic test, the properties of the contact between the drop plate and the disc shape sample were established so as it results in the same laboratory impact force on the sample. Table 2 also summarizes the micro-properties used for the dynamic drop test calibration. In all of these numerical simulations, rock failure and cracking is explicitly simulated as a bond breakage between the rigid circular particles. Figure 1 shows the BPM samples before and after static and dynamic tests. In this figure, the micro-cracks are presented in red color.

Simulation of jointed rock mass

Once the static and dynamic properties of the intact rock were simulated and calibrated, these properties were used to develop large-scale jointed rock mass samples. The size of rock mass samples was selected as 2 m width x 1 m height. This size was chosen such that the effect of reflected stress waves from the boundaries of the rock mass samples would be neglected. To investigate the influence of the joint intensity on the impact-induced damage and fragmentation of rock, discrete joint networks with different intensities were incorporated into the bonded particle model. This allowed the generation of 2D synthetic rock mass (SRM) samples in which the bonded particle model represents the rock material properties and a smooth-joint contact model (SJM) simulates the joint network, (Mas Ivars et al., 2008). In this study the joint intensity (P_{21}) is defined as the cumulated length of joint per total area of rock block.

For this investigation, three discrete joint networks with joint intensity (P_{21}) of 1, 2, and 3 m^{-1} and with the same micro-mechanical properties were considered. The joints were assigned a normal and shear stiffness of 10^{11} and 10^{10} N/m, respectively. Zero cohesion and a friction angle of 30^o were assigned to the joint surfaces.

Impact induced fragmentation of jointed rock mass samples

Using the generated SRM samples, numerical impact tests were conducted to investigate the influence of the joint intensity on the damage and fragmentation inflicted by impact load. A 0.4 m diameter rock fragment with the density of 2700 kg/m^3 was generated above the rock mass samples. It was projected vertically against the SRM samples with an impact velocity of 15 m/s (Fig. 2a). Figure 2b presents the generated SRM samples with different joint intensity.

Figure 3 shows the impact-induced damage created on the rock mass samples with different joint intensity. For comparison, the damage inflicted on the large-scale intact rock sample with no joint is presented in Fig. 3a. The results of numerical impact tests demonstrate that a crater zone is created in the area of impact. Below this crater zone, the rock material is significantly crushed. The size of the crushed zone is almost the same for all rock mass samples (~0.2 m). Beyond the crushed zone, the rest of impact energy has created large radial and wing cracks. Both shear and tension micro-cracks were generated within the rock mass samples due to impact load. The majority of these micro-cracks were generated in tension. The relationship between the number of impact-induced micro-cracks and the rock mass joint intensity is presented in Figure 4. The figure shows that increasing the joint intensity (P_{21}), up to a certain level, results in development of more micro-cracks due to impact. However, almost the same numbers of micro-cracks have developed for the rock mass samples with P_{21} of 2 and 3 m^{-1}.

Figure 5 presents the rock fragmentation analysis for the three jointed rock mass samples with different joint intensity. Impact of the projectile particle with the jointed rock mass samples creates different patterns of micro-crack in each sample, depending on their joint intensity. For the rock mass samples with higher joint intensity, the crack pattern becomes wider and deeper and consequently, results in creation of more rock fragments. For the rock mass sample with a low joint intensity, P_{21} = 1 m^{-1}, crack propagation terminates against the pre-existing joint below the damage zone. For the two rock mass samples with higher joint intensity, P_{21} = 2 and 3 m^{-1}, other cracks radiate from the initial radial cracks or from pre-existing joint surfaces, creating more damage to the samples. These cracks propagate almost perpendicular to pre-existing joint surface.

Energy transformation during the impact test of rock mass samples

The impact of the projectile particle on jointed rock mass samples can be evaluated using an energy approach. For this purpose, different forms of energy were tracked during the impact loading of SRM samples. When the projectile particle impacts the jointed rock masses, it loses significant part of its kinetic energy. Thus, there is a balance between the magnitude of kinetic energy that the projectile particle loses during the impact and the amount of energy that is absorbed by the jointed rock mass samples. The amount of dissipated energy depends on the properties of rock mass and impact conditions. The dissipated energy is stored in the synthetic rock mass blocks as strain energy, within the contact points between the circular particles. The maximum strain energy in the rock mass is reached when the projectile particle attains its largest penetration into the rock mass. The stored strain energy is transformed into other forms of energy in the rock mass including cracking, damping and dashpot energy. The dashpots energy loss is associated with the interaction between the projectile particle and the rock mass sample. The damping loss energy is related to the damping factor assigned to the particles constituting the rock mass sample. Finally, cracking energy loss is the energy that causes failure of bonds between circular particles in the rock mass sample. The maximum cracking energy loss occurs when the kinetic energy of the projectile particle is minimum. When the projectile particle is fully rebounded from the surface of rock mass sample, almost all the stored strain energy has transformed to other forms of energy. Figure 6 shows the energy transformation during the impact on the SRM sample with the joint intensity of P_{21}=1 m^{-1}.

Figure 7a shows the track of kinetic energy for the SRM samples. The figure demonstrates that more impact energy is dissipated in the SRM samples with higher joint intensity. Tracking of the cracking energy loss also supports this finding that as the joint intensity (P_{21}) of rock mass samples increases, more micro-cracks are initiated and propagated due to impact (see Fig. 7b). This can be attributed to the fact that pre-existing joint surfaces are acting as an interface from which impact-induced stress waves can reflect. This reflection results in development of more cracks in the rock mass samples.

CONCLUSIONS

The distinct-element code (PFC2D) was used to investigate the effect of joint intensity on the impact-induced damage and fragmentation of jointed rock masses. Three synthetic rock mass (SRM) samples with different joint intensity were subjected to an impact load from a rigid projectile particle. The impact-induced micro-cracks initiated and propagated into the SRM sample due to the impact load were recorded and the energy transformation during the impact tests were tracked for all the tested samples. The large-scale SRM samples were generated based on the results of laboratory tests carried out on a Meta-sandstone intact rock samples. The bonded particle model was used to simulate the static and dynamic mechanical properties of the intact rock.

The results of impact simulation for the SRM samples suggest that the presence of pre-existing joints in rock can influence the propagation of impact-induced stress wave and impact energy dissipation in rock mass. Reflection of the impact-induced stress waves from the joint surfaces can develop tensile waves in the rock mass and change the crack pattern within the rock mass. As the joint intensity in the rock mass samples increases, the regions of the rock mass carry tensile stress waves (reflected from the joints surfaces) will decreases which results in more micro-cracks nucleation, propagation and coalesce in the rock mass. This can lead in more damage to the rock mass. The results also show that for rock mass samples with lower joint intensity, the impact-induced radial cracks are generally arrested by the pre-existing joints. These radial cracks propagate almost perpendicular to the joint surface.

The study helps to better understand the damage and fragmentation mechanisms of jointed rock masses subjected to impact loads. Investigation of rock mass response to dynamic impact loading allows for a better understanding of energy dissipation in drilling and blasting process and consequently a more reliable prediction of rock fragmentation.

ACKNOWLEDGEMENTS

The authors would like to acknowledge the contribution of the CanmetMINING Rock Mechanics Laboratory, National Resources Canada, and the financial support provided by the Connaught Early Research Award, University of Toronto, Toronto, Canada.

REFERENCES

- Ahrens, T.J. and Rubin, A.M., 1993. Impact induced tensional failure in rock. *Journal of Geophysical Research*. 98(E1): 1185-1203.
- Beus, MJ.., Iverson, S.R., Dreschler, A., and Scott, V.A., 1999. Static and dynamic loads in ore and waste rock passes in underground mines. Rock Mechanics for Industry, in *Proceedings of the 37th U.S. Rock Mechanics Symposium*, Vail, Colorado, June 6-9, 1999, Netherlands: A. A. Balkema Publishers.
- Camacho, G.T, and Ortiz, M., 1996. Computational modeling of impact damage in brittle materials. *International Journal of Solids and Structures*. 33(20–22): 2899-2938.
- Cao, P., Wang, Y. and Xia, K. 2011. Testing study on damage fracture responses of rock under dynamic impact loading. *Advanced Materials Research*. Volumes 255-260, Pages 1815-1819.
- Cook, N.G.W., Hood, M and Tsai, F. 1984. Observations of crack growth in hard rock loaded by an indenter. *Int. J. Rock Mech. Min. Sci. & Geomech. Abst.* 21(2): 97–107.
- Gao, F., Hou, H., and Yang, X. 2010. Numerical analysis of dynamic mechanical properties for rock sample under strong impact loading. *Int. J. Info. Eng. Elect. Busin.* Volume 2, Pages 10-16.
- Grady, D.E., and Kipp, M. E. 1980. Continuum modeling of explosive fracture in oil shale. *Int. J. Rock Mech. Min. Sci. & Geomech. Abst.* 17(3): 147–157.
- Han, G., Bruno, M, and Grant, T. 2005. Dynamically modeling rock failure in percussion drilling. In *Proceedings of the 40th rock mechanics symposium*, Anchorage, Alaska, paper ARMA/USRMS 05-819.
- Hu, L., and Li, X. 2006. Damage and fragmentation of rock under experiencing impact load. *Journal of Central South University of Technology*, 13(4): 432−437.
- Hustrulid,W.A, and Fairhurst, C. 1972. A theoretical and experimental study of the percussive drilling of rock. Part III: experimental verification of the mathematical theory. *Int. J. Rock Mech. Min. Sci. & Geomech. Abst*. 9(3): 417–418.
- Itasca Consulting Group. 2013. Particle Flow Code, PFC2D-V.5.0. *Itasca Consulting Group, Inc*.

- Kumano, A., 1980. An experimental and analytical investigation of the response of rock to impact loading. PhD thesis, University California, Berkeley, CA.
- Kuszmaul, J.S., 1987. A new constitutive model for fragmentation of rock under dynamic loading. In *Proceedings of the Second International Symposium on Rock Fragmentation by Blasting*. Keyston CO. Pages 412-423.
- Lindqvist, P.A., 1982. Rock fragmentation by indentation and disc cutting—some theoretical and experimental studies. PhD thesis, Lulea University of Technology, Sweden.
- Lindqvist, P.A., Suarez del Rio, L.M., Montoto, M., Tan, X., and Kou, S. 1994. Rock indentation database-testing procedures, results and main conclusions. SKB Project Report 44-94-023, Sweden.
- Liu, H.Y., 2004. Numerical modeling of the rock fragmentation process by mechanical tools. PhD Thesis: 32D, Lulea University of Technology, Sweden.
- Mas Ivars D., Potyondy D.O., Pierce M., Cundall P.A., 2008. The smooth-joint contact model. In *Proceedings of the 8th World Congress on Computational Mechanics/ 5th European Congress on Computational Mechanics and Applied Science and Engineering*, Venice, Italy, Paper A2735.
- Mishnaevsky Jr , L.L. 1995. Physical mechanisms of hard rock fragmentation under mechanical loading: a review. *Int. J. Rock Mech. Min. Sci. & Geomech. Abst*. 32(8): 763–766.
- Momber, A.W., 2003. Damage to rocks and cementitious materials from solid impact. *Rock Mech. Rock Eng*. 37(603): 57-82.
- Nariseti, C., Mohanty, B., and Keskiniva, M., 2012. Crack formation in rocks due to action of cemented carbide bits. In Proc. 10th Int. Symp. on Rock Fragmentation by Blasting., Singh and Sinha (Eds.); p. 55-64.
- Nazeri, H., Mustoe, G.G.W., Rozgonyi, T. G., Wienecke, C. J., 2002. Implementation of a discrete element methodology for the modeling of gravity flow of ore in ore passes. In *Proceedings of the 5th North American Rock Mechanics Symposium and 17th Tunneling Association of Canada*, Toronto, Canada, July 7-10.
- Pang, S.S., Goldsmith, W., 1990. Investigation of crack formation during loading of brittle rock. *Rock Mech. Rock Eng*. Volume 23, Pages 53–63.
- Potyondy, D., Cundall, P.A., 2004. A bonded particle model for rock. *Int. J. Rock Mech. Min. Sci.* Volume 41, Pages 1329-1364.
- Potyondy, D.O., 2012. A flat-jointed bonded-particle material for hard rock. In *Proceedings of the 46th U.S. Rock Mechanics/Geomechanics Symposium*, Chicago, USA, June 24–27, 2012, ARMA 12-501.
- Prasad, U., Mohanty, B., and Nemes, J., 2000. Dynamic strength and fragmentation of selected rocks under impact loading. In Proc. Of 4th North Amer. Rock Mech. Symp., Girard et al., Ed., p. 577-582.
- Taylor, L. M., Chen, E. P., Kuszmaul. J. S., 1986. Microcracking-induced damage accumulation in brittle rock under dynamic loading. *Computer Methods in Applied Mechanics and Engineering*. 55(3): 301-320.
- Thorne, B.J., Hommert, P.J., Brown, B., 1990. Experimental and computational investigation of the fundamental mechanisms of cratering. In *Proceedings of the 3rd International Symposium on Rock Fragmentation by Blasting*, Brisbane, Queensland, Australia.
- Wagner, H., Schumann, E.R.H., 1971. The stamp-load bearing strength of rock–an experimental and theoretical investigation. *Rock Mech. Rock Eng.* 3(4): 185–207.
- Wang, J.K., Lehnhoff, T.F., 1976. Bit penetration into rock: a finite element study. *Int. J. Rock Mech. Min. Sci. & Geomech. Abst*. 13(1): 11–16.
- Wang, Y., Tonon, F., 2010. Discrete element modeling of rock fragmentation upon impact in rock fall analysis. Rock Mech. Rock Eng. 44(603): 23-35.

FIGURE CAPTIONS

FIG 1 – Simulated intact rock samples for the UCS, Brazilian tensile strength, and Drop test; a) before and b) after failure.

FIG 2 – a) Impact test on jointed rock mass samples, b) Simulated rock mass samples with different joint intensity.

FIG 3 – Impact induced damage within the rock mass samples with different joint intensity: (a) P_{21} =0 m^{-1}, (b) P_{21}=1 m^{-1}, (c) P_{21}=2 m^{-1}, (d) P_{21}=3 m^{-1}. Tension and shear cracks are presented in red and black, respectively.

FIG 4 – Relationship between the rock mass joint intensity and the number of impact-induced micro-cracks.

FIG 5 – Fragmentation analysis for the jointed rock mass samples.

FIG 6 – Energy transformation during the impact of the jointed rock mass sample with P_{21}=1 m^{-1}.

FIG 7 – Tracking of energy during the impact tests on the SRM samples with different joint intensity; a) Kinetic energy; b) Cracking energy.

TABLE CAPTIONS

TABLE 1. Laboratory Test Results for Meta-sandstone Rock Samples

TABLE 2. Macro-properties of the drop plate and micro-properties of the contact between drop plat and the sample.

TABLE 3. Micro-properties of the bonded particle model.

TABLE 4. Comparison between the results of laboratory tests and the BPM numerical simulations.

FIGURES

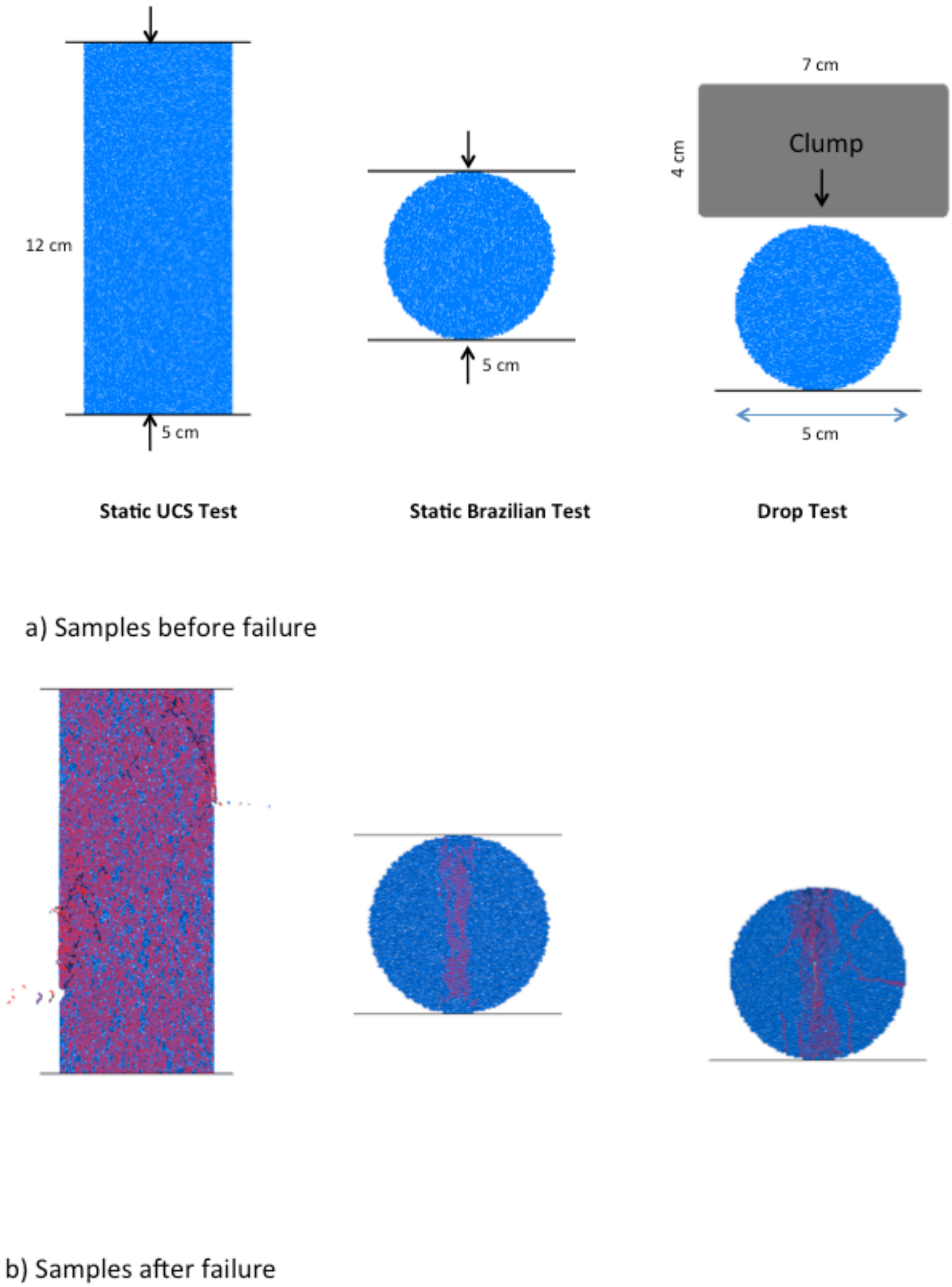

FIG 1 – Simulated intact rock samples for the UCS, Brazilian tensile strength, and Drop test; a) before and b) after failure.

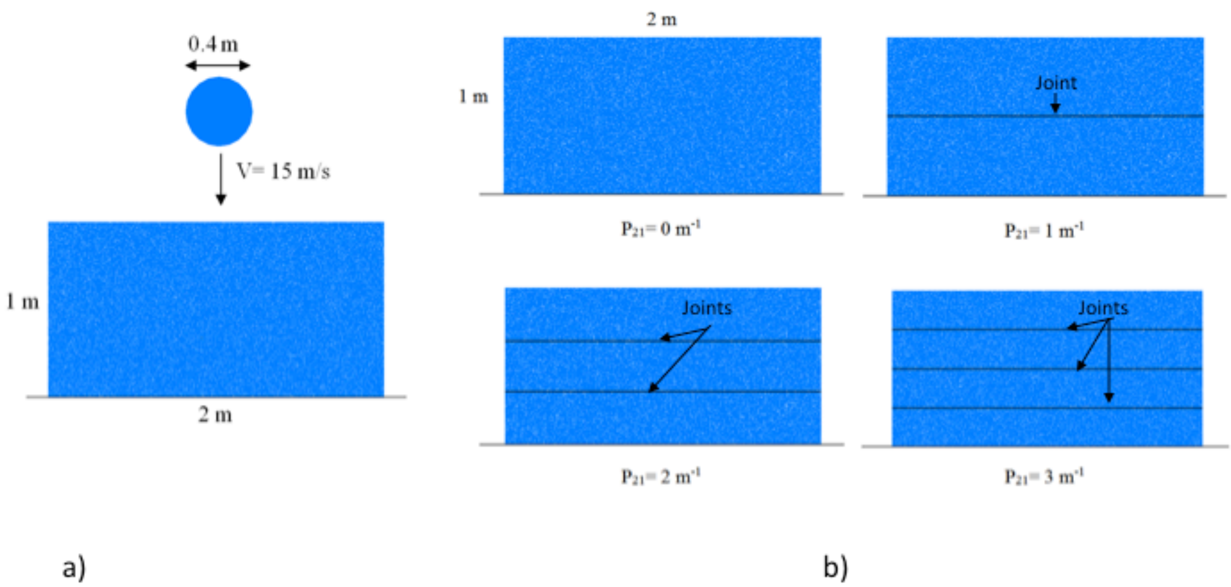

FIG 2 – a) Impact test on jointed rock mass samples, b) Simulated rock mass samples with different joint intensity.

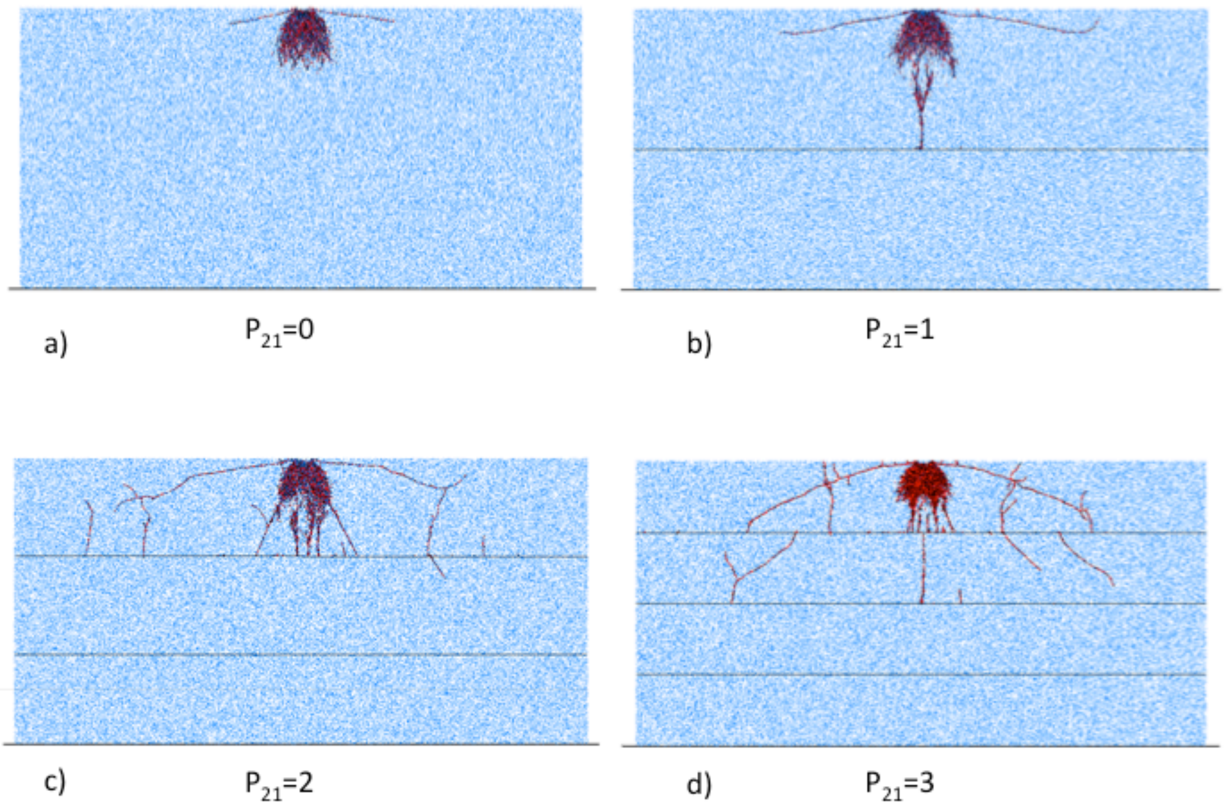

FIG 3 – Impact induced damage within the rock mass samples with different joint intensity: (a) P_{21} =0 m^{-1}, (b) P_{21}=1 m^{-1}, (c) P_{21}=2 m^{-1}, (d) P_{21}=3 m^{-1}. Tension and shear cracks are presented in red and black, respectively.

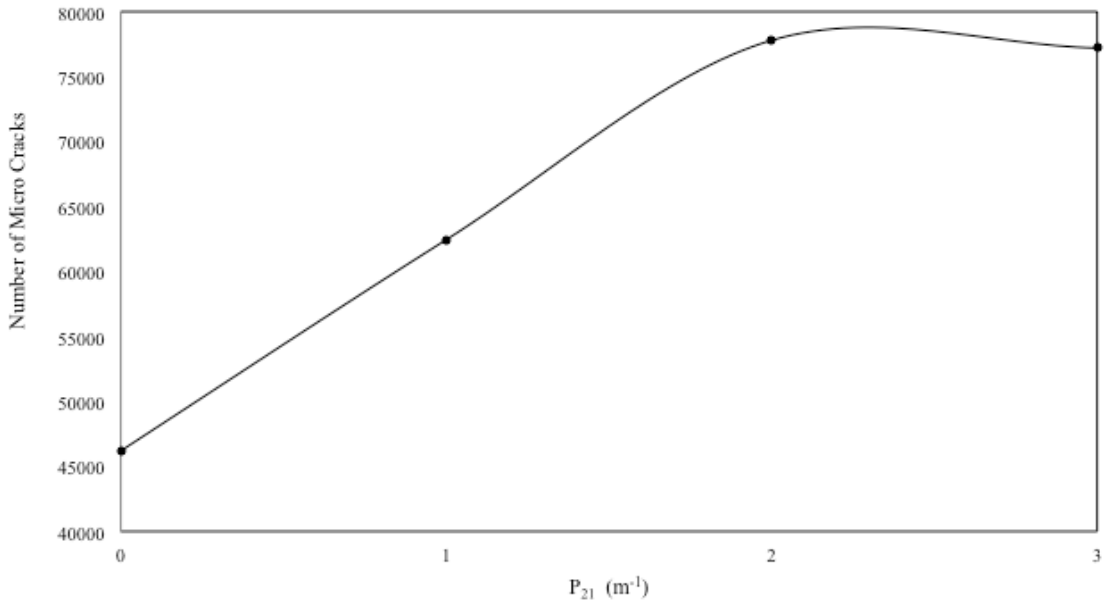

FIG 4 – Relationship between the rock mass joint intensity and the number of impact-induced micro-cracks.

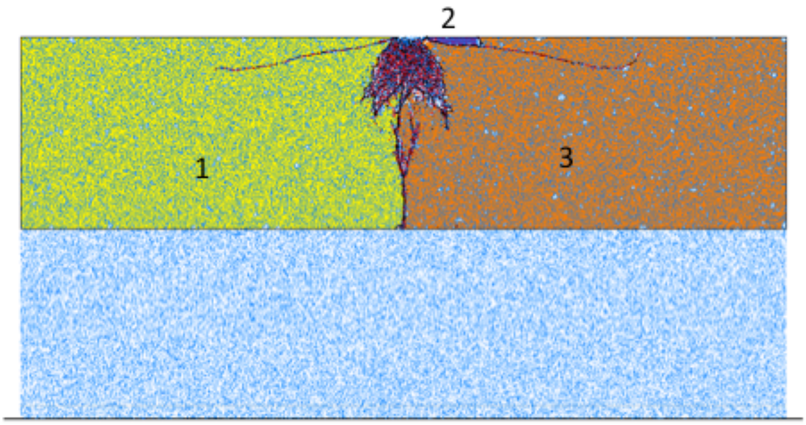

Fragment ID	Area (m^2)
1	0.4650
2	0.0024
3	0.4654

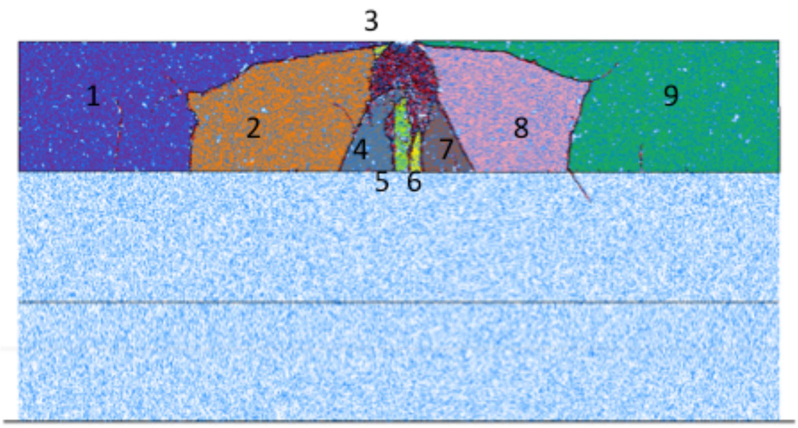

Fragment ID	Area (m^2)
1	0.1852
2	0.0705
3	0.0009
4	0.0195
5	0.0065
6	0.0031
7	0.0146
8	0.1049
9	0.2016

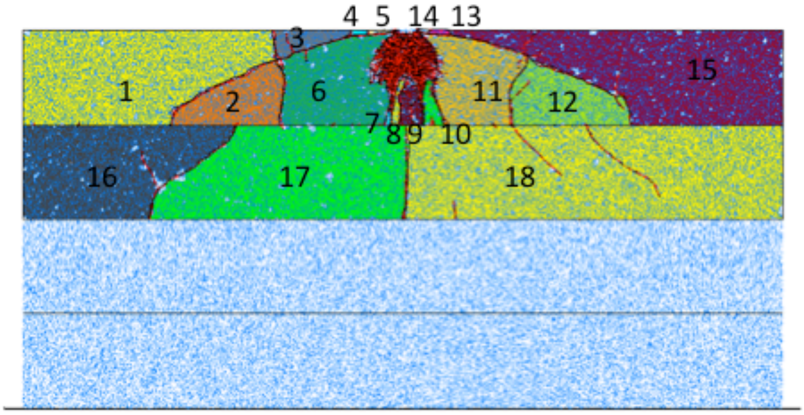

Fragment ID	Area (m^2)
1	0.1363
2	0.0332
3	0.0094
4	0.0006
5	0.0004
6	0.0566
7	0.0003
8	0.0016
9	0.0061
10	0.0040
11	0.0456
12	0.0385
13	0.0006
14	0.0003
15	0.1451
16	0.1079
17	0.1424
18	0.2478

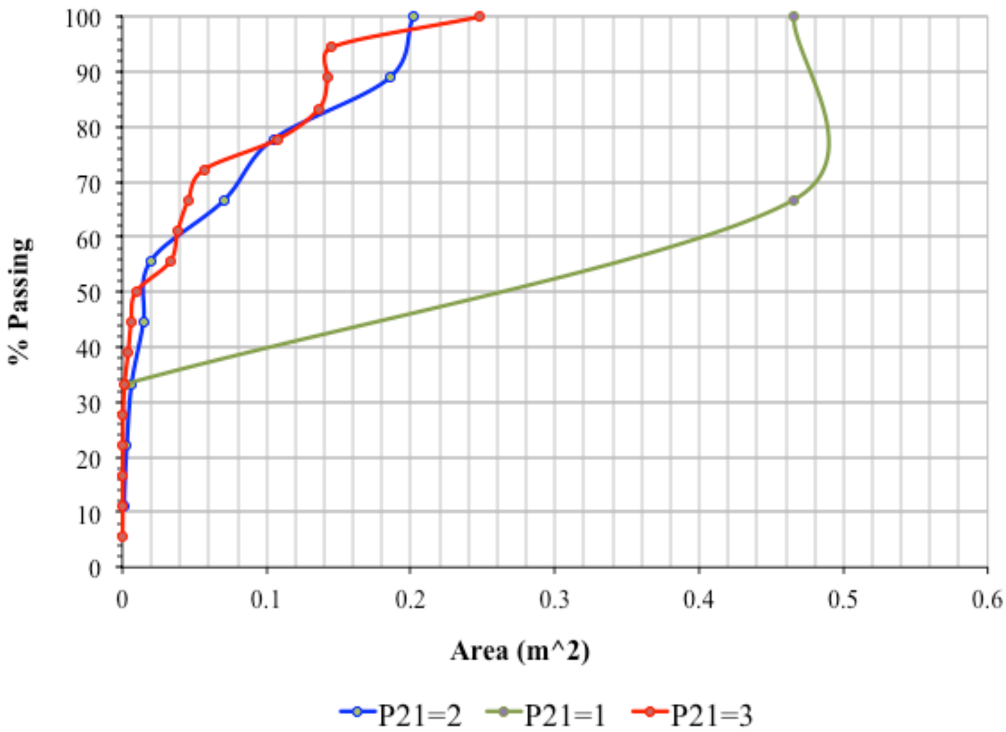

FIG 5 – Fragmentation analysis for the jointed rock mass samples.

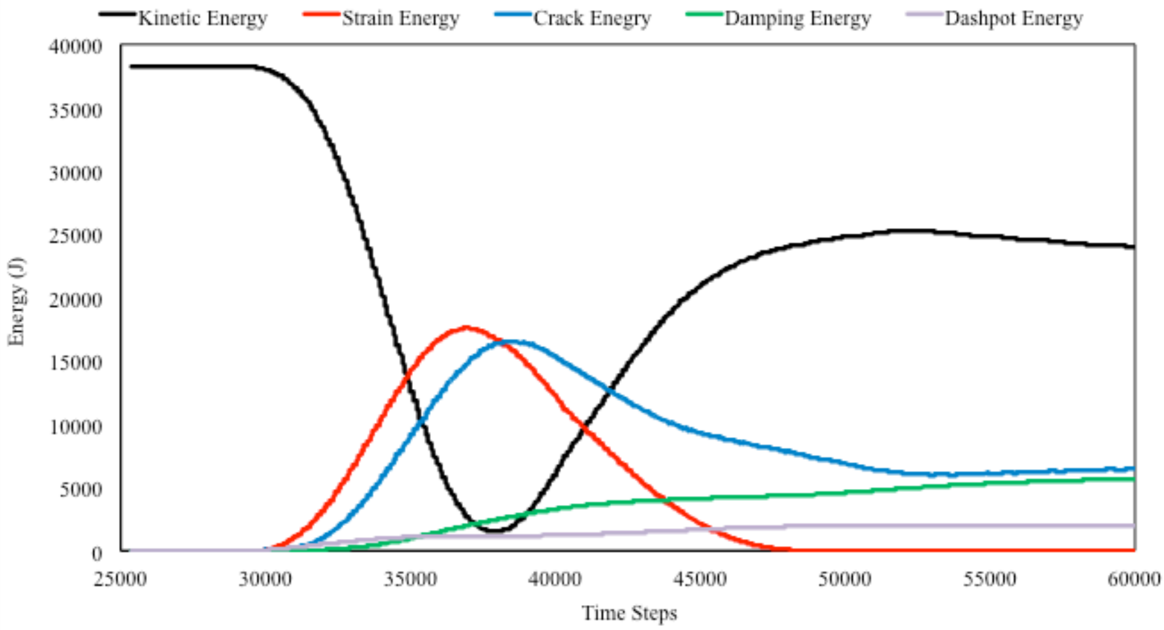

FIG 6 – Energy transformation during the impact of the jointed rock mass sample with P_{21}=1 m^{-1}.

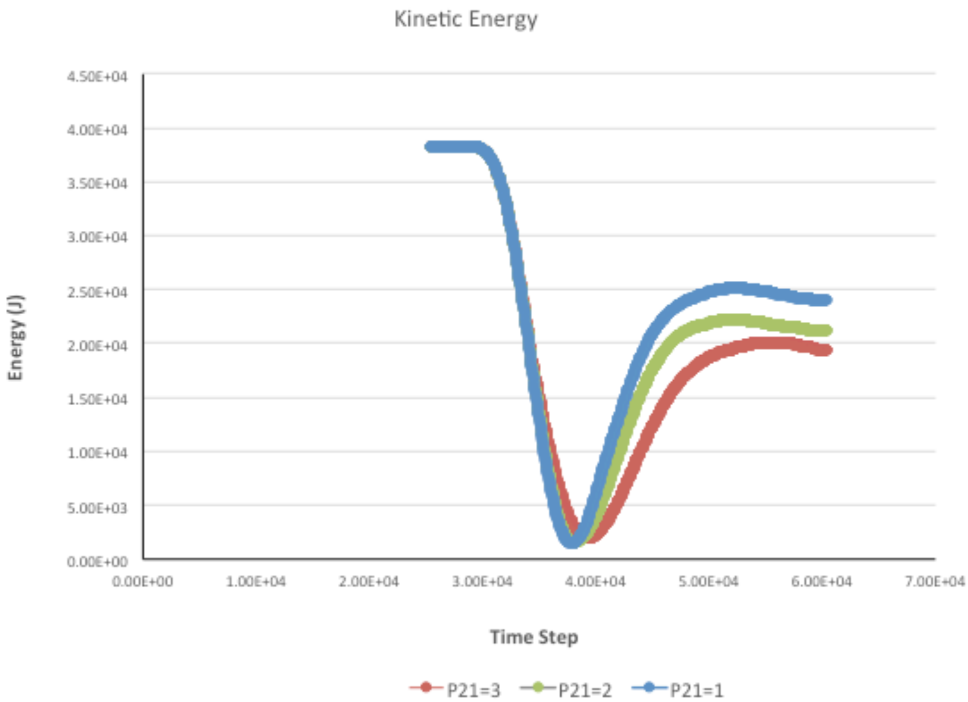

a)

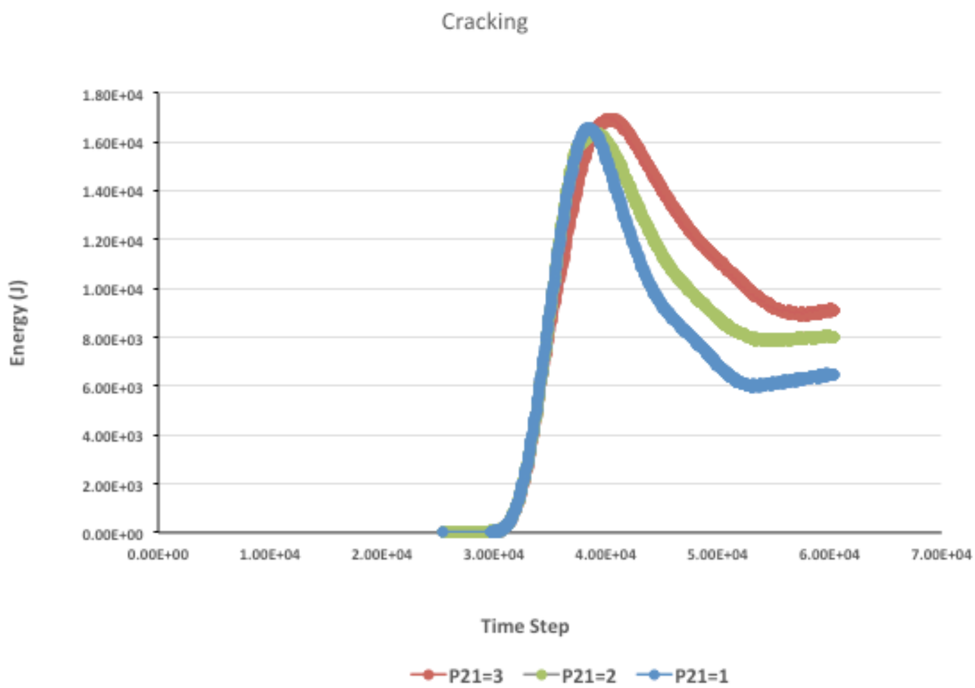

b)

FIG 7 – Tracking of energy during the impact tests on the SRM samples with different joint intensity; a) Kinetic energy; b) Cracking energy.

TABLES

TABLE 1

Laboratory Test Results for Meta-sandstone Rock Samples.

Type of Test	No. of Samples	Properties	Mean	S.D.
Uniaxial compression test	18	Elastic modulus (GPa)	74.5	5.0
		Poisson's ratio	0.26	0.10
		Axial strain at Peak (%)	0.397	0.11
		UCS (MPa)	267.0	64.0
Static Brazilian test	21	Static tensile strength (MPa)	21.5	3.0
Drop test	44	Dynamic tensile strength (MPa)	29.8	5.0
		Time to max load (ms)	0.168	0.03
		Deflection (mm)	0.491	0.09

TABLE 2

Macro-properties of the drop plate and micro-properties of the contact between drop plat and the sample.

Clump properties for simulating the drop plate		Micro-properties of the contact between the drop plate and the BPM	
Local damping factor	0.1	Normal damping ratio	1
Weight	617 kg/unit	Shear damping ratio	1
Impact velocity	3 m/s	Elastic Modulus (GPa)	60
Normal to shear stiffness ratio	1	Normal to shear stiffness ratio	1
Friction coefficient	0.5	Normal damping ratio	1

TABLE 3

Micro-properties of the bonded particle model.

Ball Properties	Density (Kg/m^3)		2713
	Minimum radius (mm)		0.3
	Maximum to minimum radius ratio		1.66
	Local Damping Factor		0.1
Contact Properties	Contact gap (m)		0.5e^{-4}
	Elastic modulus (GPa)		65
	Normal to shear stiffness ratio		3.3
	Friction angle (º)		0
	Tensile strength (MPa)	Mean	35
		S.D	25
	Cohesion (MPa)	Mean	120
		S.D	50

TABLE 4

Comparison between the results of laboratory tests and the BPM numerical simulations.

Test	Mechanical Property	Experimental	BPM	Error %
Uniaxial compression test	E (GPa)	74.5	74.9	0.5
	Poisson's ratio	0.26	0.24	7.7
	Axial strain (%)	0.397	0.404	1.8
	UCS (MPa)	267	270	1.1
Static Brazilian test	Static tensile strength (MPa)	21.4	22.3	4.2
	UCS/Tensile strength	12.5	12.1	3.2
Drop test	Max load (KN)	68.5	71.7	4.7

	Dynamic tensile strength (MPa)	29.82	30.3	1.7